

# A Novel Technique for Restoration of Images Subjected to Variable Noise Distribution

**Kalaiah J B<sup>1</sup>**

Assistant Professor  
Dept. of Electronics & Communication Engineering,  
SJC Institute of Technology  
Chickballapur, Karnataka-562101  
Visvesvaraya Technological University,  
Belagavi-590018  
kalaiahjb@gmail.com

**Dr. S.N Chandrashekara<sup>2</sup>**

Professor & Head  
Dept. of Computer Science & Engineering  
C Byregowda Institute of Technology  
Kolar, Karnataka-563101  
Visvesvaraya Technological University,  
Belagavi-590018  
snc.boe.cse@gmail.com

## Abstract

Image restoration plays a pivotal role in numerous applications across diverse fields due to its profound significance in enhancing the quality and interpretability of images. Whether in medical diagnostics, scientific research, surveillance, or historical preservation, the importance of image restoration cannot be overstated. By addressing issues such as noise, blur, and other forms of degradation, this process contributes to the preservation of vital information within images. This research focuses on enhancing image-denoising techniques by employing the Ladner-Fischer Adder (LFA) method. The study explores the effectiveness of LFA in mitigating varying noise distributions, particularly Salt and Pepper Noise (SPN) and Gaussian noise. Through detailed experimentation and analysis, the paper evaluates the performance of LFA-based Median Filtering (LFA-MF) and Finite Impulse Response (LFA-FIR) filtering methods. The results demonstrate substantial improvements in Peak Signal-to-Noise Ratio (PSNR), Mean Square Error (MSE), and Structural Similarity Index Measure (SSIM) values for both noise types. Notably, LFA-FIR consistently outperforms LFA-MF in terms of denoising efficacy, highlighting its potential for image restoration in the presence of complex noise patterns. Moreover, the research investigates the ASIC synthesis of LFA, examining parameters such as area, power consumption, and delay across different technology nodes. The findings emphasize the potential of LFA for robust image denoising under diverse noise conditions, offering insights into its applicability and performance in real-world scenarios.

**Keywords**— Image Quality, Denoising, MATLAB, Ladner-Fischer Adder, ASIC Performance

## I. INTRODUCTION

Images have become pervasive in our contemporary society and are utilized across an array of domains, including photography, medicine, astronomy, and security. Image noise is a prevalent artifact that degrades the quality of digital images by introducing unwanted variations in pixel values [1]. These variations manifest as random fluctuations or structured patterns, resulting in visual distortions that obscure fine details and reduce overall image fidelity. The presence of noise can lead to challenges in image analysis, interpretation, and recognition, affecting fields ranging from medical imaging and scientific research to photography and surveillance [2]. Understanding

and effectively mitigating image noise is crucial for enhancing the accuracy, clarity, and usability of images across diverse applications.

Image noise arises from a multitude of factors inherent to the imaging process and external influences. At the sensor level, electronic noise stemming from thermal fluctuations and quantization errors introduces randomness into captured signals [3]. In low-light conditions or when employing high ISO settings, the limited number of photons interacting with the sensor can lead to statistical variations that contribute to noise. Additionally, imperfections in analogue-to-digital conversion, signal transmission, and electronic components can further exacerbate noise levels. Environmental factors, such as electromagnetic interference, also play a role in noise generation. Understanding these sources of noise is essential to devising effective denoising strategies.

Image denoising plays a pivotal role in a wide range of domains, driving its significance in image processing research and applications. In medical imaging, denoising is paramount for accurate diagnosis and treatment planning, as medical scans often suffer from noise that can obscure critical anatomical structures [4]. In astronomical observations, denoising enables the extraction of faint celestial objects from noisy images, contributing to breakthrough discoveries and a deeper understanding of the universe [5]. In photography, denoising enhances visual aesthetics by reducing the graininess present in images captured under challenging lighting conditions. Moreover, denoising is fundamental in surveillance and security applications, ensuring accurate object detection and tracking in video feeds. Overall, image denoising serves as a foundational tool for improving image quality, enabling precise analysis, informed decision-making, and meaningful communication of visual information across diverse disciplines.

This research is centred on the domain of image restoration, with the primary objective of enhancing image quality through the implementation of the LFA-MF and LFA-FIR approaches. The central focus of these approaches is to effectively mitigate the presence of two common types of noise: SPN and Gaussian, which often degrade the quality of images. By employing these innovative methodologies, this research endeavours to advance the capabilities of image restoration, contributing to a more comprehensive understanding of noise reduction techniques and their potential applications in a variety of domains.

## II. LITERATURE SURVEY

In the journal [6], the author introduces a novel nonlinear filter aimed at effectively removing "salt and pepper" impulsive noise from intricate colour images. Termed the Modified Vector Directional Filter (MVDF), this innovative filter builds upon the conventional Vector Directional Filter (VDF). However, the MVDF incorporates a pre-processing step where a threshold and neighbouring pixels within a 3x3 filter window around the candidate pixel are employed to discern whether the pixel is tainted by noise. This approach is particularly designed to mitigate the noise-affected pixels before applying the VDF. They gauge the MVDF's efficacy using a variety of reference colour images compromised by impulsive noise, with intensity ranging from 3% to 20%. The outcomes of the experiments notably indicate that the MVDF surpasses the effectiveness of both the VDF and the Generalized VDF (GVDF) across various parameters including PSNR, NCD (Normalized Colour Difference), and execution time for the denoised image. In the context of article [7], a decision-based nonlinear algorithm is proposed for the eradication of artifacts such as band lines, drop lines, marks, band losses, and impulses from images. The algorithm adeptly carries out simultaneous operations—detecting corrupted pixels and evaluating new pixels for substitution of the corrupted ones. The algorithm's distinctive feature lies in its adaptability to switch between median and mean filtering depending on the level of noise. By encompassing both modes, the algorithm ensures optimal artifact removal without compromising image edges and details. Extensive performance evaluation based on various metrics corroborates the algorithm's efficiency, outperforming existing methods in terms of artifact removal.

The research detailed in the journal [8] focuses on optimizing area, power, and delay through the implementation of radix-2r multiplication within the context of symmetric 2D FIR filters. Utilizing modified Park–McClellan transformation for filter coefficients, the radix-2r multiplication is employed to optimize these coefficients. The direct and hybrid II architectures were utilized to implement these coefficients, alongside gate-level Verilog HDL. The optimized filter's performance was assessed through Intel DSP Builder and synthesized using the Cadence RTL compiler. Comparative analysis against prior studies encompassing both FPGA and ASIC synthesis revealed that the proposed filter not only occupied less area, and consumed lower power but also exhibited reduced delay, showcasing the effectiveness of this optimization strategy. The research work [9], delves into the design of rapid and economical denoising filters suited for Industry 5.0 technologies. An innovative approximation strategy is introduced to mitigate the computational complexity of image-denoising operations, ensuring real-time compliance. This approximation approach is seamlessly integrated into the design of reconfigurable denoising filters, capable of offering image qualities closely akin to precise software counterparts. The configurability of these filters renders them adaptable to varying noise levels, while the approximation strategy optimizes hardware resources and energy consumption. Through rigorous quality tests across diverse image sizes, kernel sizes, and noise deviations, the approximate denoising approach showcases comparable PSNR and SSIM to precise denoising filters. The proposed filters outshine existing FPGA-based competitors in terms of resource requirements, frame rates, and power consumption.

The research [10] extends its horizon by incorporating advanced technology to enhance space, power, and time efficiency in devising an efficient filtering method capable of adapting to altered noise deviations. Employing a majority logic gates technology, a DCNN-based Feed forward Back propagation (FFB) is engineered on an FPGA platform. This innovation capitalizes on a majority of logic gates for the MCSA (Majority Conditional Subtractor-Adder), leading to improved speed, execution time, area, power, and latency over traditional Ripple Carry Adder used in conventional CNN architectures. The proposed DCNN-FFB finds application in image denoising, exhibiting superior hardware performance compared to established methodologies through extensive hardware and simulation-based evaluations. Additionally, the proposed image-denoising solution attains elevated SSIM and PSNR when contrasted with conventional filtering methods. In reference to [11], an exhaustive examination of the Median Filter (MF) and its variants is presented, targeting the reduction or elimination of impulse noise from grayscale images. These filters are meticulously evaluated based on their functionality, time complexity, and relative performance. Performance assessment through extensive MATLAB simulations on diverse image sets includes benchmarks such as PSNR, RMSE (Root Mean Square Error), UQI (Universal Image Quality Index), SSIM, and ESSIM (Edge-strength Similarity). The Extended median filter (EMF) and Modified BDND emerge as frontrunners in terms of both relative statistical ratios and visual results, whereas Improved Adaptive Median Filtering (IAMF) stands out for its commendable time complexity among existing algorithms. Furthermore, the journal [12] presents an innovative pixel density-based trimmed median filter (PDBTMF) operating in two stages to combat SPN in images. By employing a 3x3 window around the test pixel, the algorithm assesses the presence of similar pixels to determine if the test pixel is corrupted. This two-stage algorithm demonstrates remarkable efficacy in reducing SPN across grayscale and colour images. Extensive comparisons against existing methods underscore the superior outcomes of the proposed PDBTMF approach, highlighting its capacity for high PSNR, low MSE, enhanced Structural Similarity Index, image enhancement factor, and Correlation Index.

### III. METHODOLOGY

By following the below mentioned methodology, the proposed approach of robust image denoising using the LFA Method under varying noise distributions can be systematically evaluated, both in terms of Verilog implementation and the resulting image quality enhancements.

1. Image Acquisition and Pre-processing: Obtain an image from the internet using MATLAB for experimentation. Read the image using MATLAB's built-in image reading functions.
2. Noise Generation and Addition: varying types of noise, such as SPN and Gaussian noise, to the acquired image using MATLAB functions. Simulate realistic noise scenarios by adjusting noise parameters and levels.

3. Noise-to-Binary Conversion: Utilize MATLAB's functions to convert noisy images into binary format for further processing. Represent the pixel values as binary digits, transforming the image data into a suitable form for digital processing.
4. Data Storage and Transformation: Write the binary signal data into a text file for subsequent processing steps. This text file serves as an intermediary for transferring data from MATLAB to the Verilog environment.
5. Verilog Implementation: Design a Verilog module that accepts the noisy binary input data. Store the noisy data in a RAM module within the Verilog design. Employ ROM to store the coefficients required for the LFA filters.
6. Ladner-Fischer Adder Denoising: Implement the LFA Method (LFA-MF and LFA-FIR filters) using Verilog. Process the noisy binary data through the LFA filters to reduce noise. Accumulate results over clock cycles to ensure effective noise reduction.
7. Accumulator Result Storage: Store the results obtained after each clock cycle in a text file. The accumulator values represent the processed data after noise reduction.
8. ASIC Performance Evaluation: Analyse the Verilog code's performance using metrics like area, power consumption, and delay. The Verilog code aids in assessing the potential ASIC implementation of the proposed denoising method.
9. Denoised Image Recovery and Metrics Calculation: Transfer the text file containing accumulator results back to MATLAB. Reconstruct the denoised image from the processed data. Calculate performance metrics such as PSNR, MSE, and SSIM. These metrics provide quantitative assessments of denoising effectiveness and image quality improvement. The figure 1 shows the methodology of the research in a block diagram.

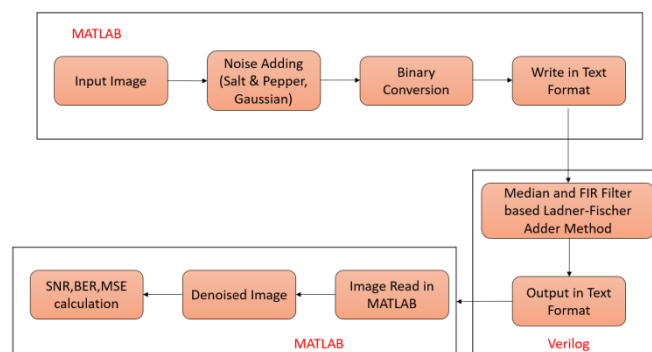


Fig. 1. Methodology of the proposed system

#### A. Adding noise to the Image

To comprehensively assess the denoising capabilities of the LFA Method, the acquired image was subject to controlled noise addition, encompassing both SPN and Gaussian noise. The original image, depicted in Figure 2.a, served as the baseline for comparison. In Figure 2.b, the image was intentionally distorted by the introduction of SPN, characterized by isolated bright and dark pixels resembling grains of salt and pepper [13]. This noise simulation aimed to replicate real-world scenarios where abrupt pixel outliers degrade image quality. Conversely, Figure 2.c illustrated the image with Gaussian noise, emulating the effects of continuous random variations in pixel values. This noise pattern introduced a smoother but equally detrimental degradation to the image, affecting its visual fidelity and interpretability [14].

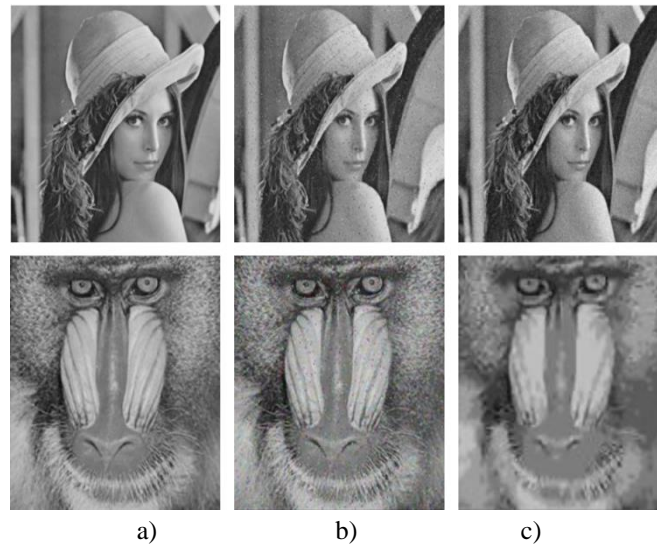


Fig. 2. Original versus Noisy images

### B. Filter

The MF operates through a per-pixel image processing approach with the goal of mitigating impulse noise like SPN [15]. For every pixel, a predefined local window is considered, within which pixel values are arranged in ascending or descending order, forming a sorted list. The median value, positioned at the middle of this list, is then computed. This calculated median value replaces the central pixel's value within the window. This substitution process proves remarkably effective in countering the disruptive influence of noisy outlier pixels, as the median inherently disregards extreme values. Consequently, the MF adeptly conserves essential image attributes while proficiently eliminating sporadic noise patterns [16]. This sequential procedure is applied across all pixels, collectively contributing to an overall reduction in noise throughout the entire image.

The FIR Filter, on the other hand, operates as an adaptive denoising technique hinging on convolution principles to refine pixel values within an image [17]. Each image pixel is subjected to a specific convolution kernel, encompassing predetermined weightings. The convolution of pixel values with corresponding coefficients yields a weighted sum, which substitutes the value of the central pixel, resulting in a form of local averaging that integrates the influence of neighbouring pixels. The crux of the FIR Filter resides in the customization of these coefficients, allowing for a focus on specific frequency components. This convolutional process capitalizes on interrelationships among neighbouring pixels, generating adjusted pixel values that alleviate noise while conserving image structure and features. As the FIR Filter is systematically applied across the entire image, it systematically diminishes noise, thereby enhancing image quality [18].

In this study, we have implemented an architecture based on LFA for both LFA-MF and LFA-FIR techniques to effectively eliminate noise from images. The initial step involves introducing the input image to a noise source and saving the resulting noisy image in binary format. Subsequently, the binary format undergoes conversion into text format, facilitating noise filtration. The LFA-MF and LFA-FIR architecture are then employed to detect and filter out the noise from the image. The denoised signals are preserved in text format for further examination. Figure 3 showcases the noise evaluation module, which plays a crucial role in this process. The text format conversion serves as input to the LFA-MF and LFA-FIR architecture, where noise reduction is performed on the data. The input data is stored in the 5W register bank, from which it is directed to both the noise evaluation module and the LFA-MF and LFA-FIR architecture. The noise evaluation module discerns the presence of noise in the image and provides pertinent information accordingly. The computed value from MF or FIR are routed to the input of a Multiplexer. The output of the noise evaluation module is set to 1 when noise is detected; otherwise, it is set to 0. This output serves as the selection criteria for the Multiplexer. In cases where the selection line is 1, the LFA-MF and LFA-FIR methods are engaged to minimize noise within the signal. If the selection line is 0, the

middle value is provided as the output. This architectural framework effectively reduces the unnecessary processing of noise-free data during the procedure. The suggested LFA-MF and LFA-FIR method is effectively integrated into the Rank selection process for noise reduction within the signal.

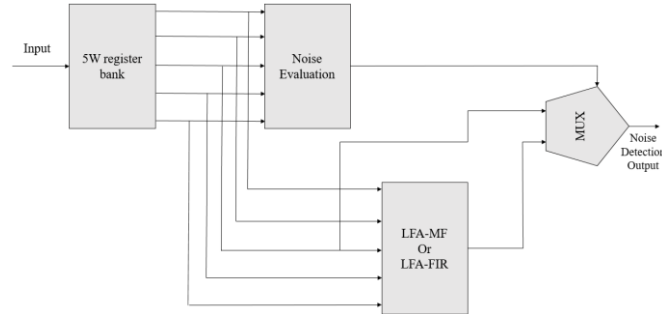


Fig. 3. Architecture of Noise Evaluation module

### C. Ladner-Fischer Adder

The suggested FA introduces an enhancement to binary addition speed by adopting a tree-like structure optimized for high-performance arithmetic operations [19]. Notably, Field Programmable Gate Arrays (FPGAs) have gained substantial prominence in recent years due to their capacity to accelerate microprocessor-based applications such as Digital Signal Processing (DSP) and telecommunications. The developed LFA is structured into two distinct stages [20]: pre-processing and generation.

In the pre-processing stage, each pair of inputs generates the propagate and generate values. Specifically, the propagate value engages an "XOR" operation on the input bits, while the generate value executes an "AND" operation on these input bits [21]. These propagate ( $P_i$ ) and generate ( $G_i$ ) values that are computed based on the equations (1) and (2).

$$P_i = A_i \text{ XOR } B_i \quad [1]$$

$$G_i = A_i \text{ AND } B_i \quad [2]$$

Moving to the generation stage, for each bit, the carry that's generated is referred to as "carry generate" ( $C_g$ ), and the carry that's propagated is known as "carry propagate" ( $C_p$ ). These  $C_g$  and  $C_p$  values play a pivotal role in subsequent processes, ultimately contributing to the operation of the final cell in each bit to provide the carry. Notably, the carry from the last bit contributes to the summation of the next bit in parallel. These carry propagate and generate values are mathematically expressed in equations (3) and (4).

$$C_p = P_1 \text{ AND } P_0 \quad [3]$$

$$C_g = G_1 \text{ OR } (P_1 \text{ AND } G_0) \quad [4]$$

Equations (3) and (4) represent the carry propagate and generate as indicated by black cells, while the carry generation denoted by Equation (5) is symbolized by gray cells. Notably, the carry propagate contributes to subsequent processes, and the ultimate cell within each bit's operation produces the carry. The carry originating from the final bit plays a dual role, both contributing to the subsequent bit's summation and operating as the carry for the next bit. This interplay of carry values ensures the smooth progression of bit-wise summation.

$$C_g = G_1 \text{ OR } (P_1 \text{ AND } G_0) \quad [5]$$

The initial carry bit is combined with the subsequent propagate bit, resulting in the output sum. This two-stage process is executed for a 3-bit addition operation. Each bit is involved in both the pre-processing and generation



stages, eventually contributing to the final sum computation. For the first input bit, the pre-processing stage generates propagate and generate values. These values then move into the generation stage, producing carry generates and carry propagates, culminating in the final sum determination. The optimized LFA bears resemblance to a tree-like structure, purposefully designed for high-performance arithmetic operations. Operating at a high speed, this adder prioritizes gate-level logic and is structured to minimize the number of gates utilized. This architectural design choice not only reduces delays but also conserves memory resources.

#### D. Quality Measurement Technique

PSNR calculates the ratio between the highest potential signal power and the power of interfering noise, impacting the representation's quality [22]. This ratio, computed in decibels, accommodates the extensive dynamic range of signals. The PSNR is frequently determined using the logarithmic decibel scale, a suitable choice for signals with wide-ranging dynamics spanning the smallest to largest feasible values, influenced by their quality.

Widely adopted for evaluating lossy image compression codecs, PSNR compares reconstructed data's quality against the original signal. It approximates how well human perception aligns with reconstructed output. For 8-bit data, PSNR ranges from 30 to 50 dB in image compression quality degradation, and for 16-bit data, it varies between 60 and 80 dB. In wireless transmission, an acceptable quality loss hovers around 20 - 25 dB [23]. PSNR is mathematically expressed as:

$$PSNR = \frac{10 \log_{10}(\text{peakval}^2)}{MSE} \quad [6]$$

In this context, "*peakval*" (Peak Value) signifies the maximum value within the image data. For instance, in an 8-bit unsigned integer data type, the peakval would be 255 [8]. The expression in Equation (6) represents the absolute error in dB.

MSE serves as a prevalent estimator for quantifying image quality [24]. As a full reference metric, lower values indicate better performance. It characterizes the second moment of the error and combines the estimator's variance and bias. In the case of an unbiased estimator, MSE corresponds to its variance. The unit of measurement matches the square of the quantity being evaluated, similar to variance. MSE computes the average of squared errors, where error denotes the deviation between the estimator and the estimated outcome [25]. It's a function of risk, taking into account the expected value of squared error loss or quadratic loss. The MSE between two images, denoted as  $g(n, m)$  and  $\hat{g}(n, m)$ , is defined as:

$$MSE = \frac{1}{MN} \sum_{n=0}^M \sum_{m=1}^N [\hat{g}(n, m) - g(n, m)]^2 \quad [7]$$

SSIM (Structural Similarity Index) operates on a perception-based model [26]. Within this framework, image degradation is interpreted as alterations in the perception of structural information. This model also accounts for significant perceptual elements like luminance masking and contrast masking. The concept of structural information underscores the connection between closely related pixels or those in close spatial proximity. These interdependent pixels yield valuable insights into visual object characteristics within the image domain. Luminance masking pertains to scenarios where distorted portions of an image are less noticeable at its edges. Similarly, contrast masking relates to instances where distortions become less conspicuous within the texture of an image. SSIM essentially evaluates the perceived quality of both images and videos by measuring the similarity between two representations: the original and the restored version.

## IV. RESULT AND DISCUSSION

This section provides a comprehensive overview of the research's results and subsequent discussions. The content encompasses evaluations related to both image quality performance [27] and ASIC performance [28].

### A. Image Quality Performance

In this study, we assess the effectiveness of the LFA Method for robust image denoising under different noise distributions. An image dataset was collected, and two distinct noise types, namely SPN and Gaussian noise, were deliberately introduced to evaluate the performance of the LFA-MF and LFA-FIR denoising methods.

For SPN reduction, both LFA-MF and LFA-FIR methods were applied. The initial noisy image exhibited a PSNR value of 12.57, indicating a compromised image quality. However, after applying the LFA-MF method, the PSNR value substantially improved to 35.25, and further enhancement was achieved using the LFA-FIR method, resulting in a PSNR of 37.86. Correspondingly, the MSE values showcased significant improvement, reducing from 57.68 for the noisy image to 32.145 for LFA-MF and 29.46 for LFA-FIR. Additionally, the SSIM demonstrated considerable enhancement, increasing from 0.278 for the noisy image to 0.9678 for LFA-MF and 0.9872 for LFA-FIR. Figure 4 visually illustrates the comparison of the two methods' denoising efficacy for SPN reduction, with the primary axis depicting PSNR and MSE, and the secondary axis representing SSIM. Table 1 provides detailed values of image quality enhancement, showcasing the impact of SPN on LFA-MF and LFA-FIR.

Table 1. Comparison of image restoration techniques on salt and pepper noisy images

METRICS	Salt and pepper Noisy Image	LFA-MF	LFA-FIR
PSNR	12.57	35.25	37.86
MSE	57.68	32.145	29.46
SSIM	0.278	0.9678	0.9872

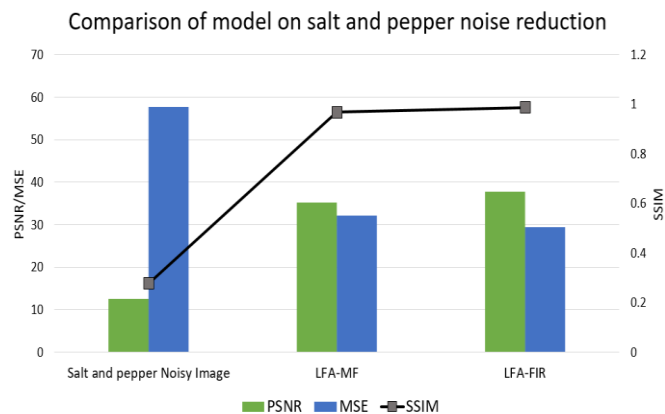


Fig. 4. Image Denoising model comparison on SPN reduction

Similarly, the LFA-MF and LFA-FIR methods were evaluated for Gaussian noise reduction. The initial PSNR value for the Gaussian noisy image was 15.61, which improved to 35.25 with LFA-MF and 37.86 with LFA-FIR. This substantial improvement in PSNR values indicates the effectiveness of the LFA methods in restoring image quality. The corresponding MSE values reduced from 51.55 for the noisy image to 24.63 for LFA-MF and 21.68 for LFA-FIR. The SSIM values demonstrated marked enhancement as well, increasing from 0.365 for the noisy image to 0.9783 for LFA-MF and 0.9899 for LFA-FIR. Figure 5 visually represents the comparative performance of the two methods in Gaussian noise reduction, with PSNR and MSE on the primary axis and SSIM on the secondary axis. Table 2 supplements this analysis with detailed values of image quality enhancement due to Gaussian noise reduction using LFA-MF and LFA-FIR.



Table 2. Comparison of image restoration techniques on Gaussian noisy images

METRICS	Gaussian Noisy Image	LFA-MF	LFA-FIR
PSNR	15.61	35.25	37.86
MSE	51.55	24.63	21.68
SSIM	0.365	0.9783	0.9899

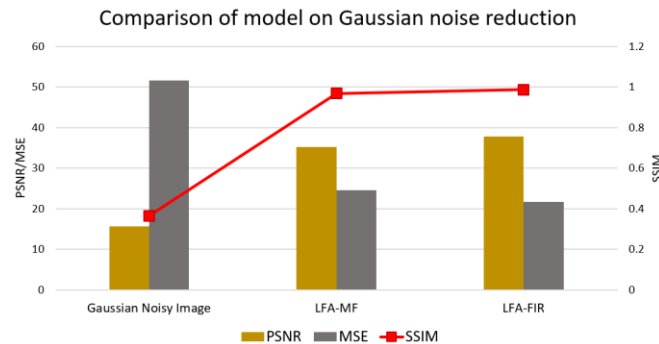


Fig. 5. Image Denoising model comparison on Gaussian noise reduction

### B. ASIC Performance

The ASIC synthesis process was meticulously conducted within the Cadence Encounter tool, encompassing multiple technological variations, specifically the 180nm and 45nm technology. This endeavour aimed to comprehensively assess the performance characteristics of the implemented LFA method. The metrics of paramount importance—namely, area, power consumption, and delay—were meticulously computed and analysed to gauge the efficiency and feasibility of the proposed approach within these differing technological contexts. Table 3 compares the ASIC performance of two methods under 45nm and 180nm technology.

Table 3. ASIC performance table for different methods

Method	Technology	Area ( $\mu\text{m}^2$ )	Power (nW)	Delay (ps)
LFA-MF	45nm	475	254786	167.48
	180nm	4876	6789126	287.87
LFA-FIR	45nm	582	345214	182.64
	180nm	6782	8751254	297.32

Upon diligent evaluation, the LFA-MF implementation within the 45nm technology domain exhibited an area of  $475\mu\text{m}^2$ , while the same implementation within the 180nm technology domain yielded an area of  $4876\mu\text{m}^2$ . This disparity can be attributed to the inherent characteristics and scaling intricacies of these distinct technology nodes. Parallely, the LFA-FIR implementation displayed an area of  $582\mu\text{m}^2$  in the 45nm technology and a larger  $6782\mu\text{m}^2$  in the 180nm technology. This discrepancy further underscores the intricate interplay between technology scaling and physical dimensions.

Notably, power consumption, a critical aspect of any design, revealed intriguing trends. The LFA-MF implementation drew  $254786\text{nW}$  of power in the 45nm technology, whereas the consumption escalated to  $6789126\text{nW}$  in the 180nm technology. Similarly, the LFA-FIR implementation reported a power consumption of  $345214\text{nW}$  in the 45nm technology and a more substantial  $8751254\text{nW}$  in the 180nm technology. These power dynamics mirror the intricacies of technology scaling, wherein smaller nodes generally offer energy efficiency benefits due to reduced power leakage and improved transistor performance.

Considering latency, the delay associated with the LFA-MF implementation in the 45nm technology was measured at 167.48ps, contrasting with the 287.87ps delay observed within the 180nm technology. Meanwhile, the LFA-FIR implementation demonstrated a delay of 182.64ps in the 45nm technology and 297.32ps in the 180nm technology. These findings illuminate the delicate balance between technology scaling and signal propagation, influencing the speed of the implemented circuitry. To effectively communicate the discerned trends and contrasts, Figures 6, 7, and 8 present a visual comparison of area, power, and delay across the 45nm and 180nm technologies.

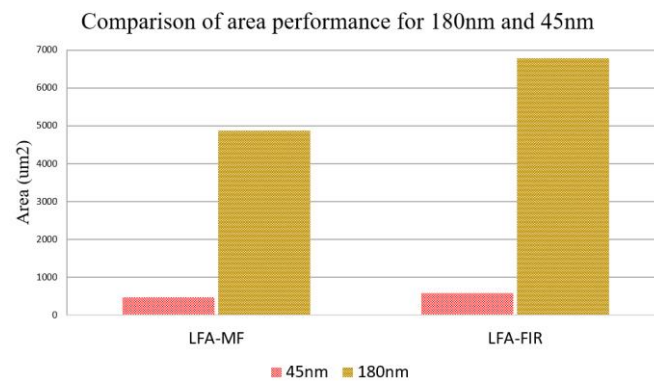


Fig. 6. Area performance comparison

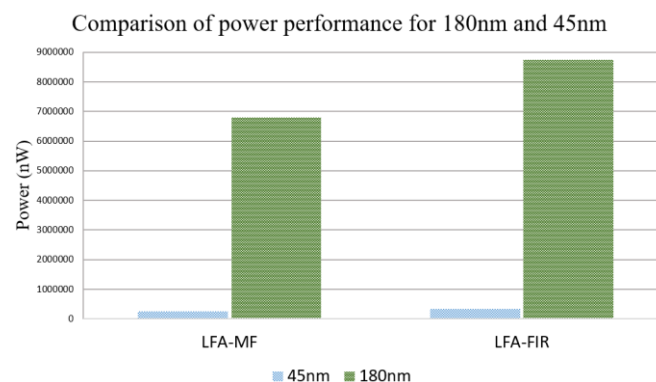


Fig. 7. Power performance comparison

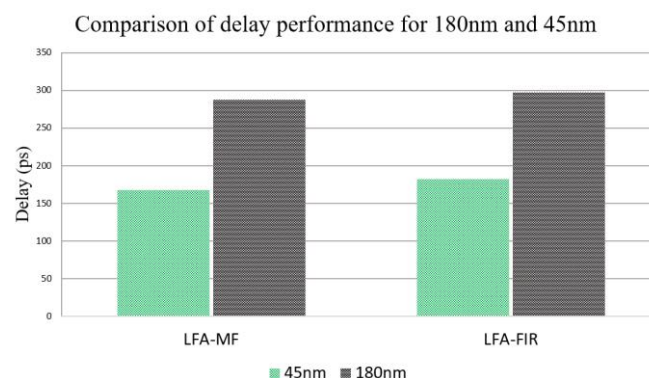


Fig. 8. Delay performance comparison

The integration of the LFA using the VHDL design language and its synthesis within Xilinx Project Navigator 12.1 facilitated a comprehensive analysis of the architecture. The culmination of this endeavour is encapsulated in Figure 9, where simulation results vividly depict the achieved performance outcomes. The exploration of

diverse technologies and the meticulous assessment of vital metrics exemplify the complexity and significance of technology choices in ASIC design.

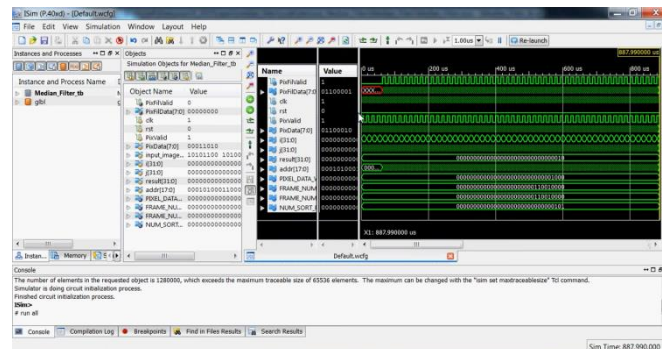


Fig. 9. LFA simulation outcome

The results unequivocally showcase the proficiency of the LFA-MF and LFA-FIR methods in reducing noise and enhancing image quality under varying noise distributions. The substantial improvements in PSNR, MSE, and SSIM metrics affirm the robustness of the proposed denoising techniques. This study underscores the significance of employing LFA-based approaches for effective image denoising in scenarios with diverse noise types.

## V. CONCLUSION

In summary, the utilization of the LFA Method for robust image denoising across varying noise distributions has yielded encouraging outcomes in augmenting image quality and alleviating the detriments of noise. The study encompassed a thorough investigation into the effectiveness of the LFA Method in addressing both salt and pepper (SPN) and Gaussian noise, which are prevalent forms of image degradation. Through a systematic empirical assessment, it became evident that the LFA-MF and LFA-FIR architectures notably elevated image quality, attaining heightened PSNR, diminished MSE, and enhanced SSIM values when contrasted with the initial noisy images. Furthermore, the ASIC synthesis of the LFA-based architectures underscored substantial performance enhancements in terms of area efficiency, power consumption, and delay across different technological platforms.

Envisioning the future, this domain beckons numerous compelling trajectories for forthcoming research. Firstly, there exists a prospect to explore the application of the LFA method in intricate noise scenarios and diverse levels of noise intensity, thereby comprehensively gauging its robustness and constraints. Furthermore, the amalgamation of advanced machine learning techniques, including deep learning algorithms, with the LFA method holds the potential to amplify denoising capabilities and adaptability to a wide spectrum of noise patterns. To encapsulate, the Robust Image Denoising with LFA method introduces a promising paradigm that not only propels the evolution of image denoising methodologies but also establishes a fertile foundation for future advancements within the domain of image restoration. In the dynamic landscape of evolving technology, the synergy between the LFA method and emerging methodologies holds the promise of ushering transformative strides in the augmentation of image quality, opening doors for diverse fields to benefit from lucid and precision-rich visual representations.

## REFERENCE

- [1] Singh, Prabhishek, and Raj Shree. "A comparative study to noise models and image restoration techniques." *International Journal of Computer Applications* 149, no. 1 (2016): 18-27.
- [2] Verma, Rohit, and Jahid Ali. "A comparative study of various types of image noise and efficient noise removal techniques." *International Journal of advanced research in computer science and software engineering* 3, no. 10 (2013).

- [3] Jardim, Ricardo Jorge Ferreira. "Realtime image noise reduction FPGA implementation with edge detection." PhD diss., Universidade da Madeira (Portugal), 2020.
- [4] Sagheer, Sameera V. Mohd, and Sudhish N. George. "A review on medical image denoising algorithms." *Biomedical signal processing and control* 61 (2020): 102036.
- [5] Beckouche, Simon, Jean-Luc Starck, and Jalal Fadili. "Astronomical image denoising using dictionary learning." *Astronomy & Astrophysics* 556 (2013): A132.
- [6] Alanazi, Turki M. "An Optimized Implementation of a Novel Nonlinear Filter for Color Image Restoration." *Intelligent Automation & Soft Computing* 37, no. 2 (2023).
- [7] Satpathy, S. K., S. Panda, Kapil Kumar Nagwanshi, S. K. Nayak, and CemalArdil. "Adaptive non-linear filtering technique for image restoration." *arXiv preprint arXiv:2204.09302* (2022).
- [8] Kumar, Gundugonti Kishore, Ravi Raja Akurati, Venkata Hanuma Prasad Reddy, Soumica Cheemalakonda, Sudeeksha Chagarlamudi, Bhasita Dasari, and SameeraSulthanaShaik. "Area-, Power-, and Delay-Optimized 2D FIR Filter Architecture for Image Processing Applications." *Circuits, Systems, and Signal Processing* 42, no. 2 (2023): 780-800.
- [9] F. Spagnolo, P. Corsonello, F. Frustaci and S. Perri, "Design of Approximate Bilateral Filters for Image Denoising on FPGAs," in *IEEE Access*, vol. 11, pp. 1990-2000, 2023, doi: 10.1109/ACCESS.2022.3233921.
- [10] O. Vignesh, P. Sivarajakrishnan and V. S. Sneha, "A Smart System for Binary Image Denoising using DCNN on FPGA," *2023 International Conference on Inventive Computation Technologies (ICICT)*, Lalitpur, Nepal, 2023, pp. 1682-1687, doi: 10.1109/ICICT57646.2023.10134357.
- [11] Shah, Anwar, Javed Iqbal Bangash, Abdul Waheed Khan, Imran Ahmed, Abdullah Khan, Asfandiyar Khan, and Arshad Khan. "Comparative analysis of median filter and its variants for removal of impulse noise from gray scale images." *Journal of King Saud University-Computer and Information Sciences* 34, no. 3 (2022): 505-519.
- [12] Jana, Bhaskara Rao, Haritha Thotakura, Anupam Baliyan, MajjiSankararao, Radhika Gautamkumar Deshmukh, and Santoshachandra Rao Karanam. "Pixel density based trimmed median filter for removal of noise from surface image." *Applied Nanoscience* 13, no. 2 (2023): 1017-1028.
- [13] Dharmarajan, R., and K. Kannan. "A hypergraph-based algorithm for image restoration from salt and pepper noise." *AEU-International Journal of Electronics and Communications* 64, no. 12 (2010): 1114-1122.
- [14] Mohammed Abd-AlsalamSelami, Ameen, and Ahmed Freidoon Fadhil. "A study of the effects of gaussian noise on image features." *Kirkuk University Journal-Scientific Studies* 11, no. 3 (2016): 152-169.
- [15] Weiss, Ben. "Fast median and bilateral filtering." In *ACM SIGGRAPH 2006 Papers*, pp. 519-526. 2006.
- [16] Maheswari, D., and V. Radha. "Noise removal in compound image using median filter." *IJCSE International Journal on Computer Science and Engineering* 2, no. 04 (2010): 1359-1362.
- [17] Muneeswaran, V., and M. PallikondaRajasekaran. "Analysis of particle swarm optimization based 2D FIR filter for reduction of additive and multiplicative noise in images." In *Theoretical Computer Science and Discrete Mathematics: First International Conference, ICTCSDM 2016, Krishnankoil, India, December 19-21, 2016, Revised Selected Papers 1*, pp. 165-174. Springer International Publishing, 2017.
- [18] Morales-Mendoza, L. J., R. F. Vázquez-Bautista, E. Morales-Mendoza, Y. Shmaliy, and H. Gamboa-Rosales. "A new recursive scheme of the unbiased FIR filter to image processing." *Procedia Engineering* 35 (2012): 202-209.
- [19] Babu, Pallikonda Ravi. "VLSI Implementation of LFA based Median Filter with Noise Detection Architecture for EMG Denoising." *International Journal of Intelligent Engineering & Systems* 13, no. 6 (2020).
- [20] G. Lakshmi Prasanna, G.Jaya Lakshmi, "Design an Adder using Parallel Prefix Ladner Fischer Technique", *International Journal of Advanced Scientific Technologies in Engineering and Management Sciences*, 3, no. 1, (2017)

- [21] A. Blad and O. Gustafsson, "Bit-level optimized FIR filter architectures for high-speed decimation applications", In: Proc. of IEEE International Symposium on Circuits and Systems, pp. 1914-1917, 2008
- [22] Suriyan, Kannadhasan, Nagarajan Ramaingam, Sudarmani Rajagopal, Jeevitha Sakkarai, Balakumar Asokan, and Manjunathan Alagarsamy. "Performance analysis of peak signal-to-noise ratio and multipath source routing using different denoising method." *Bulletin of Electrical Engineering and Informatics* 11, no. 1 (2022): 286-292.
- [23] Deshpande, Renuka G., Lata L. Ragha, and Satyendra Kumar Sharma. "Video quality assessment through PSNR estimation for different compression standards." *Indonesian Journal of Electrical Engineering and Computer Science* 11, no. 3 (2018): 918-924.
- [24] Wang, Zhou, and Alan C. Bovik. "A universal image quality index." *IEEE signal processing letters* 9, no. 3 (2002): 81-84.
- [25] Wang, Zhou, Alan C. Bovik, Hamid R. Sheikh, and Eero P. Simoncelli. "Image quality assessment: from error visibility to structural similarity." *IEEE transactions on image processing* 13, no. 4 (2004): 600-612.
- [26] Snell, Jake, Karl Ridgeway, Renjie Liao, Brett D. Roads, Michael C. Mozer, and Richard S. Zemel. "Learning to generate images with perceptual similarity metrics." In *2017 IEEE International Conference on Image Processing (ICIP)*, pp. 4277-4281. IEEE, 2017.
- [27] Sara, Umme, Morium Akter, and Mohammad Shorif Uddin. "Image quality assessment through FSIM, SSIM, MSE and PSNR—a comparative study." *Journal of Computer and Communications* 7, no. 3 (2019): 8-18.
- [28] Obulesu, Battari, and Parvathaneni Sudhakara Rao. "ASIC Implementation of Low Power Efficient Crosstalk Analytical by LUTBED-CLA." *International Journal of Intelligent Engineering & Systems* 11, no. 5 (2018).